

Supporting Information

Nanoscale Topography of Anodic TiO₂ Nanostructures Is Crucial for Cell-Surface Interactions

Jung Park,^{†,#} Alexander B. Tesler,[‡] Ekaterina Gongadze,[§] Aleš Iglíč,^{§,||} Patrik Schmuki,^{‡,⊥} and Anca Mazare^{*,‡,#}

[†]University Hospital Erlangen, Division of Molecular Pediatrics, Department of Pediatrics, 91054 Erlangen, Germany.

[‡]Department of Materials Science WW4-LKO, Friedrich-Alexander University of Erlangen Nürnberg, Erlangen, Germany.

[§]Laboratory of Physics, Faculty of Electrical Engineering, University of Ljubljana, Tržaška 25, Ljubljana, SI-1000, Slovenia.

^{||}Laboratory of Clinical Biophysics, Faculty of Medicine, University of Ljubljana, Vrazov Trg 2, Ljubljana, 1000, Slovenia.

[⊥]Regional Centre of Advanced Technologies and Materials, Czech Advanced Technology and Research Institute, Palacky University, Olomouc, 779 00, Czech Republic.

Corresponding author e-mail: anca.mazare@fau.de

1. Long-range order of the nanostructures using a two-step anodization approach

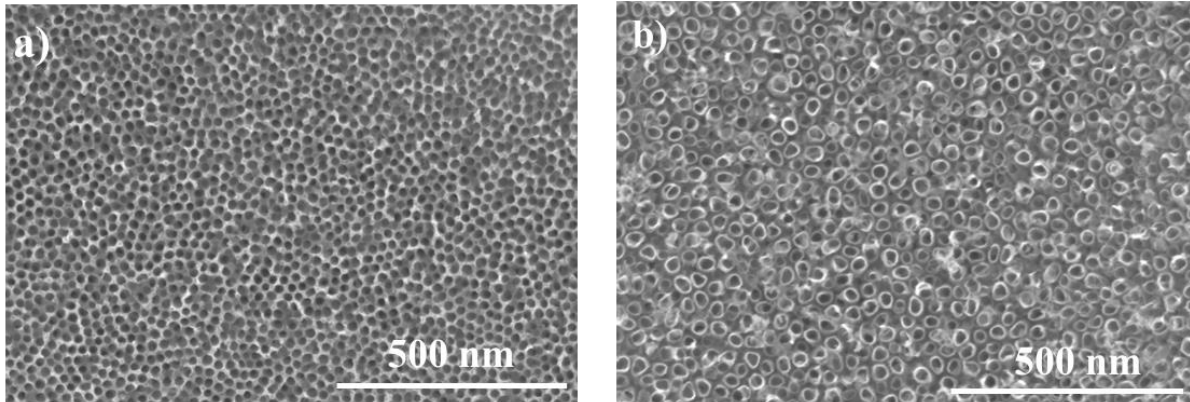


Figure S1. High-resolution SEM images of a) NPs and b) NTs showing very good long-range order.

2. Typical initiation layer-covered TiO₂ nanotubes

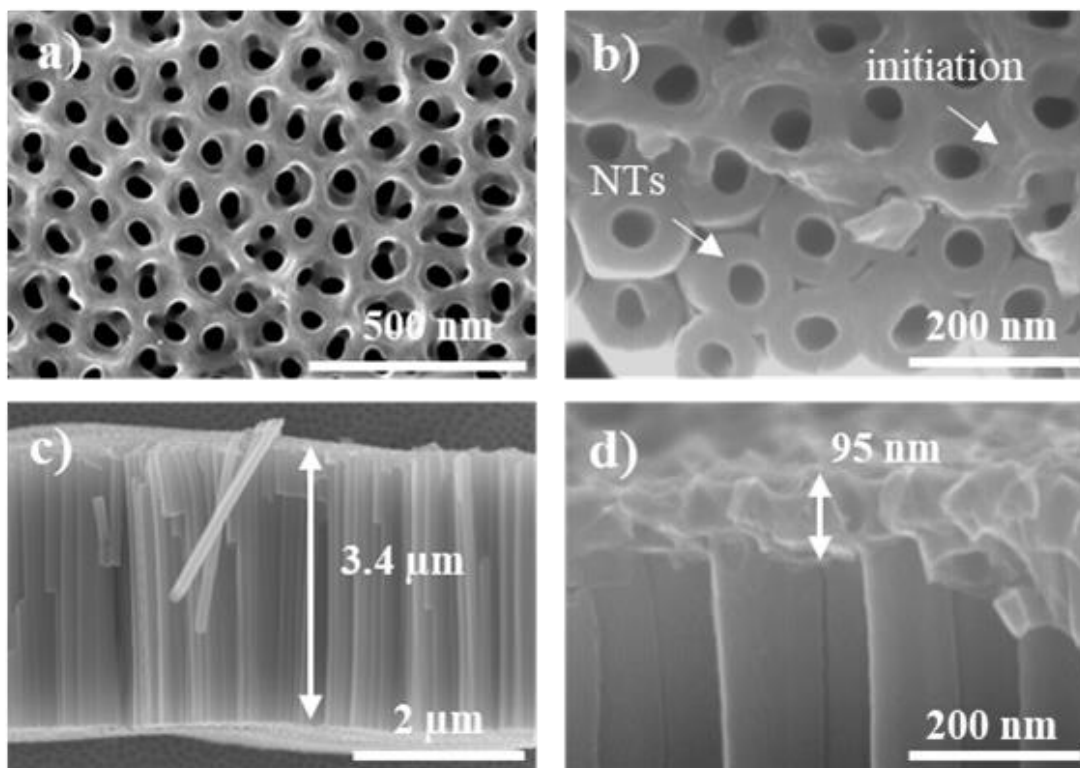


Figure S2. Typical NTs covered with a thin initiation layer obtained in ethylene glycol-based electrolytes with NH₄F (in a double anodization approach, in EG + 0.3 % w/v NH₄F + 1 % v/v H₂O, final anodization at 60 V for 10 min): (a, b) top-view SEM images, (c) cross-sectional SEM image, and (d) cross-sectional view showing the thickness of the initiation layer.

3. XRD patterns of the obtained nanostructures and of the Ti substrate

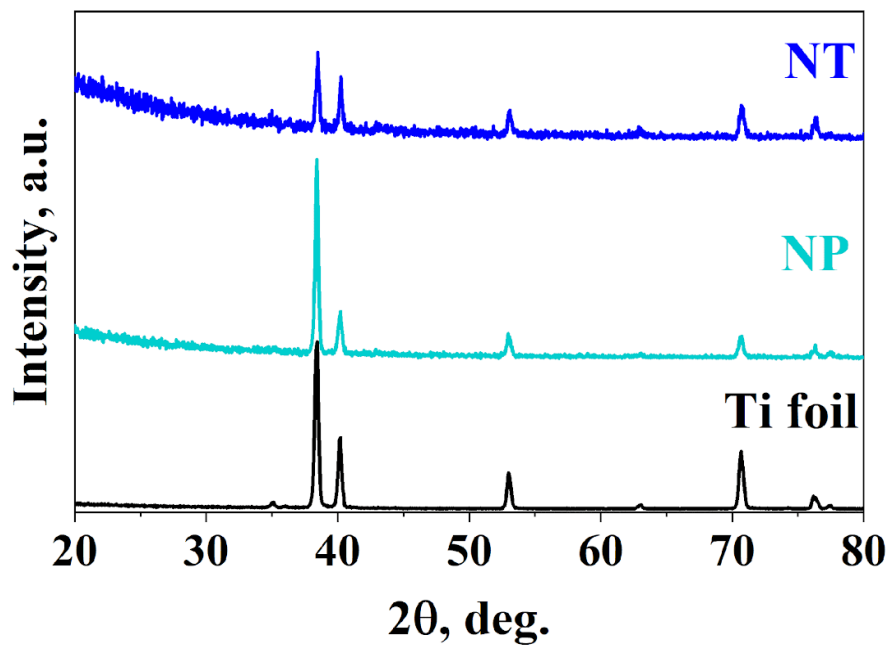


Figure S3. XRD patterns of the Ti foil, NP, and NT nanostructures show that the anodic layers are amorphous, as only the peaks of titanium (Ti foil) are observed.

4. EDX and XPS data of the NP and NT nanostructures

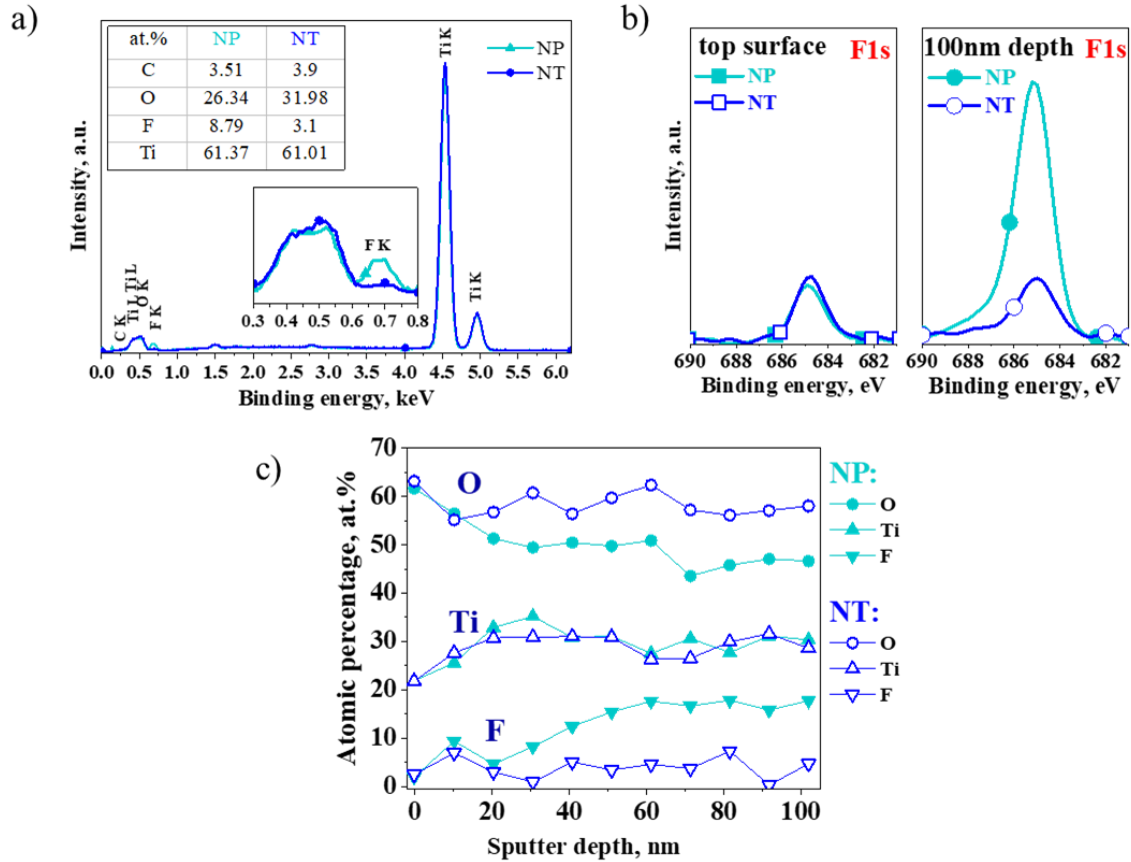


Figure S4. a) EDX spectra and at. % of the nanostructures; b) XPS high-resolution spectra of the F1s peak before and after sputtering 100nm; and c) corresponding XPS depth profiles of the first 100 nm, showing the atomic percentages of Ti, O, and F.

5. ToF-SIMS data of the NP and NT nanostructures

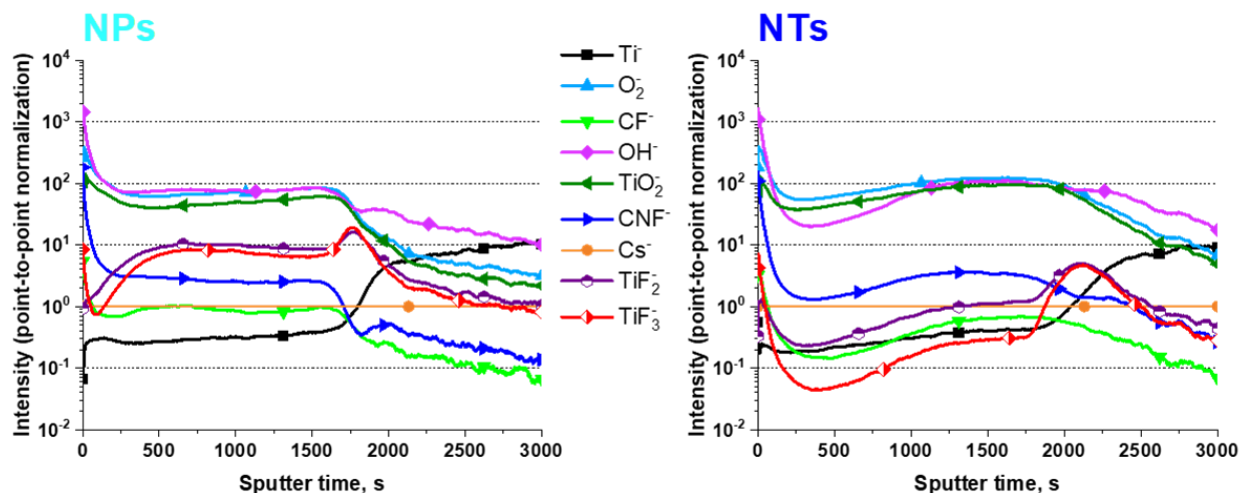


Figure S5. ToF-SIMS depth sputter profiles in the negative polarity of the NPs (left panel) and NTs (right panel) showing selected mass fragments of Ti⁻ (m/z 47.948), O₂⁻ (m/z 31.990), CF⁻ (m/z 30.999), OH⁻ (m/z 17.003), TiO₂⁻ (m/z 79.938), CNF⁻ (m/z 45.002), Cs⁻ (m/z 132.906), TiF₂⁻ (m/z 85.945), and TiF₃⁻ (m/z 104.943).

The full ToF-SIMS negative depth profile spectra with additional mass fragments are shown in **Figure S5**, and SEM images of the sputter crater are in **Figure S6**. We observe a higher intensity count for the TiF₃⁻ and TiF₂⁻ mass fragments of NPs (TiF₃⁻ in **Figure 3c**, TiF₂⁻ in **Figure S5**), but both nanostructures show for these mass fragments a bump in intensity close to the interface, which can be attributed to the pore/tube bottom at the oxide layer/metal interface. There are also differences in the distribution of the CNF⁻ mass fragment over the length, *i.e.*, for NTs in the first part of the layer, the intensity is lower. This is consistent with the more pronounced V-shape of the NTs, with a thinner tube wall at the top. In addition, the interface for NPs is at ≈ 2150 s, while for NTs is ≈ 2700 s.

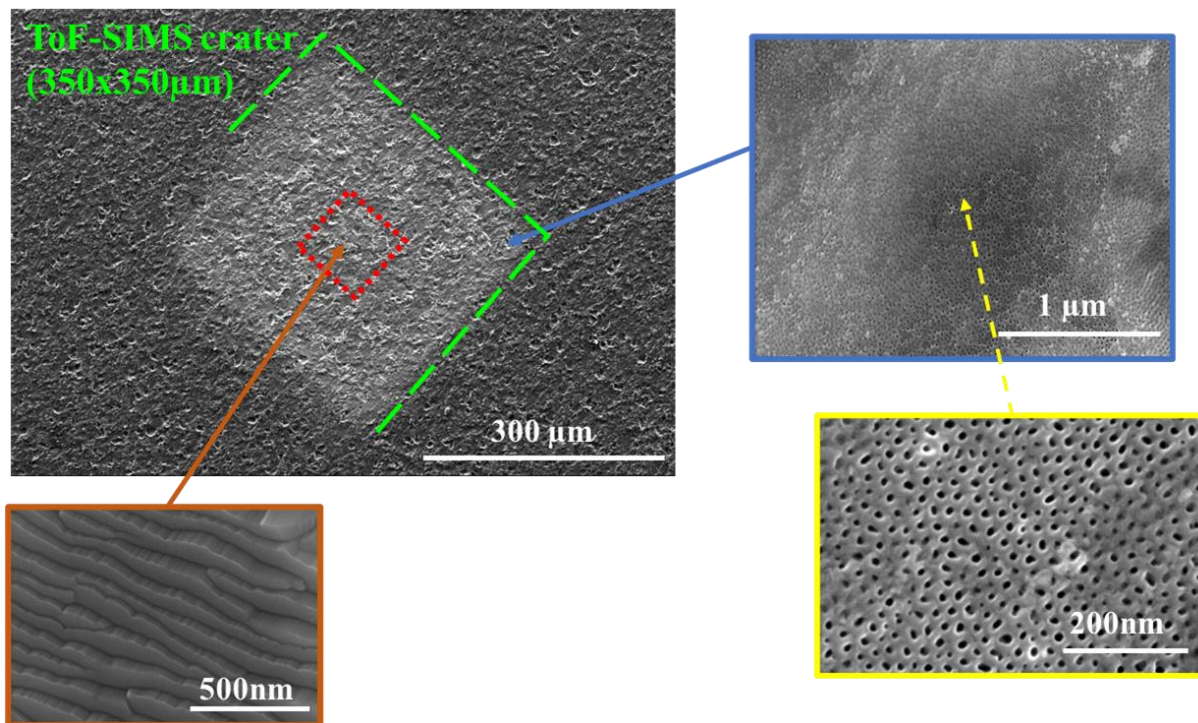


Figure S6. Example of the ToF-SIMS crater for the NPs, showing the $350 \times 350 \mu\text{m}$ sputter crater (marked with dashed green line), the measurement area of $65.6 \times 65.6 \mu\text{m}$ in the center of the sputter crater (marked with red dotted line), and high-resolution SEM images from the center of the crater, and from the edge of the sputter crater (showing the morphology of the NPs after sputtering).